Graphite Foam Heat Exchanger for Vhielces

Lin, Wamei; Sundén, Bengt

2011

[Link to publication](#)

Graphite foam heat exchanger for vehicles

W LIN, B SUNDÉN
Department of Energy Sciences, Lund University, Sweden

ABSTRACT

Because of the high thermal conductivity (1700 W/(m.K)) and the low density (0.2 to 0.6 g/cm^3), the graphite foam is a good option for heat exchangers in vehicles. However, there is a high pressure drop through the foam due to the open cells of the foam. In order to evaluate the performance of graphite foam heat exchanger, a simulation comparison between a convectional aluminum louver fin heat exchanger and a corrugated graphite foam heat exchanger is carried out in this paper. The aim of the comparison is to investigate the coefficient of performance (COP), power density (PD), and compactness factor (CF). Useful recommendations are highlighted to promote the development of graphite foam heat exchangers in vehicles.

Nomenclature

A	area (m^2)	L_f	foam walls pitch (mm)
A_b	heated base area (m^2)	L_p	louver pitch (mm)
c_p	specific heat (J.kg^{-1}.K^{-1})	L_w	louver width (mm)
C_F	Forchheimer coefficient	m	mass (kg)
CF	compactness factor (kW.m^{-3})	Nu	Nusselt number
COP	coefficient of performance	PD	power density (kW.kg^{-1})
D	length scale (m)	P_{pump}	the input power of pump (W)
D_h	hydraulic diameter (m)	$Q_{removed}$	the removed heat (W)
F_L	fin length (mm)	T_p	tube pitch (mm)
F_p	fin pitch (mm)	u	velocity (m.s^{-1})
h	heat transfer coefficient (W.m^{-2}.K^{-1})	V	the volume (m^3)
k	thermal conductivity (W.m^{-1}.K^{-1})	$\triangle T$	the temperature difference (K)

Greek Symbols

α	permeability (m^2)	ε	porosity
δ	thickness of graphite foam (mm)	μ	dynamic viscosity (Pa·s)
θ	louver angle (degree)	ρ	density (kg.m^{-3})

Subscripts

eff	effective	in	inlet
f	fluid	s	solid
HEX	heat exchanger		

1 INTRODUCTION

Due to the increased power of vehicles, the cooling problem of vehicles becomes more serious than before. An efficient cooling system is required not only to dissipate the heat from vehicles, but also to reduce the weight of the vehicle, which will lead to less fuel consumption. In order to increase the thermal performance of heat exchangers in vehicles, it is important to apply extended surfaces on the air side to compensate for the low heat transfer coefficient. However, because of space limitation in vehicles, there is not much available space to increase the size of heat exchangers. Consequently, there is a demand to develop a new compact heat exchanger with high thermal performance.

In order to develop a new compact heat exchanger, a porous medium might be a good choice as material for the heat exchangers. Even though aluminum or copper heat exchangers are common in vehicles currently, because of their high thermal conductivity. The porous medium - graphite foam, which was developed by Oak Ridge National Laboratory [1], has extremely high thermal conductivity. Several research works about the characteristics of graphite foams were carried out [2-4]. In summary, the characteristics of graphite foams are as follows:

   I.   High thermal conductivity: The effective thermal conductivity of graphite foam is between 40 and 150 W/(m.K) [4], which is much higher than the effective thermal conductivity of an aluminum foam (between 2 and 26 W/(m.K) [5]).
   II. Low density: The density of graphite foam is from 0.2 to 0.6 g/cm^3 which is about 20 % that of aluminum.
   III. Large specific surface area: Because of the open cells and inter-connected void structure, the specific surface area of graphite foam is between 5000 and 50000 m^2/m^3.
   IV. Weak mechanical properties: The tensile strength of graphite foam is much lower than that of the metal foam.

Based on these characteristics, the graphite foam is a potential material for heat exchangers. Klett et al. [6] designed a radiator with carbon foam. The cross section of the automotive radiator was reduced from 48 cm x 69 cm to 20 cm x 20 cm. The reduced size can decrease the overall weight, cost and volume of the system. Yu et al. [7] proved the thermal performance of a carbon foam finned tube radiator could be improved 15 % compared to a conventional aluminum finned tube radiator, without changing the frontal area, or the air flow rate and pressure drop. Furthermore, Garrity et al. [8] carried out an experimental comparison between the carbon foam heat exchanger and the multilouvered fin heat exchanger. When the volume of the heat exchangers was the same, the carbon foam samples brought away more heat than the multilouvered fin.

Even though there is a huge heat transfer enhancement in the graphite foam, the high pressure drop is the major issue facing the graphite foam, due to the large hydrodynamic loss associated with the cell windows connecting the pores [9]. In order to reduce the pressure drop, six different configurations of graphite foam heat exchangers were presented in [10]. The solid foam had the highest pressure drop, and the finned configuration had the lowest pressure drop. On the other hand, Leong et al. [11] found that the baffle foam presented the lowest pressure drop among the four configurations of graphite foams, at the same heat transfer rate. Lin et al. [12] proved that a corrugated

foam could reduce the pressure drop while maintaining a high heat transfer coefficient, compared to the solid foam. Thus, the configuration has an important effect on the pressure drop through the graphite foam.

According to the literature review, a corrugated graphite foam has low pressure drop and high thermal performance. However, it is still not clear whether the corrugated graphite foam has better performance than a convectional louver fin or not. In order to clarify this, a comparison between the corrugated graphite foam and aluminum louver fin is carried out in this paper. The aim of the comparison is to evaluate: (1) coefficient of performance (COP, how much heat can be removed by a certain input pump power); (2) power density (PD, how much heat can be removed by a certain mass of fins); and (3) compactness factor (CF, how much heat can be removed in a certain volume).

2   PHYSICAL MODEL AND ASSUMPTIONS

2.1   Physical model

A simplified model of a plate-fin heat exchanger is shown in Fig. 1. The corrugated graphite foam is placed between two water tubes as function of fins, as shown in Fig. 1. The fluid is assumed to be incompressible with constant properties, and the flow is steady-state. The water tubes are made of aluminum. Due to the large heat transfer coefficient between the water and the inner tube wall and the high thermal conductivity of the tube wall, the water tube is assumed to be at constant temperature. The thermal resistance between the tube wall and the graphite foam is neglected.

The overall size of the fin core is 1.2 cm (width) x 4.5 cm (height) x 5 cm (length).
- Graphite foam size: the thickness of graphite foam (δ) is 2.5 mm; and the pitch between two foam walls (L_f) is 7.5 mm.
- Louver fin size: The louver fin pitch (Lp) is 1 mm; the louver angle (θ) is 29 degree; fin pitch (Fp) is 2.5 mm.
- Parameters of the graphite foam are: Porosity (ε) is 0.82; The effective thermal conductivity (k_{eff}) is 120 W/(m.K); The permeability (α) is 6.13 x 10^{-10} m^2; The Forchheimer coefficient C_F is 0.4457.

a. Corrugated graphite foam
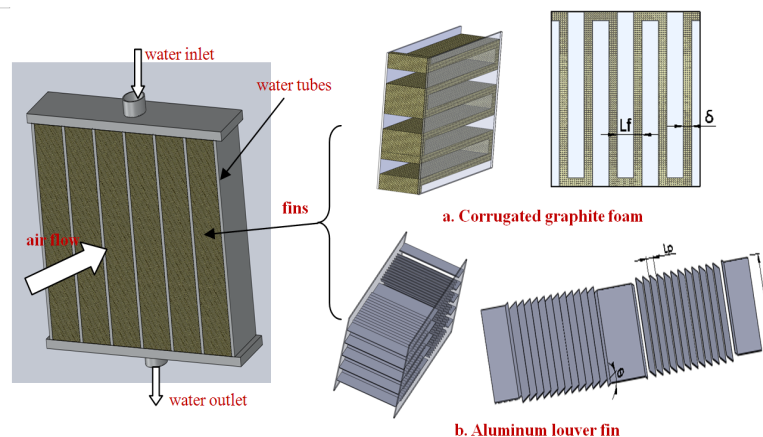
b. Aluminum louver fin

Fig. 1. Heat exchanger with (a) corrugated graphite foam and (b) aluminum louver fin.

2.2 Adoption of flow model

Before the numerical computations, a discussion of the computation model (laminar or turbulent) concerning flow regime is carried out. In the comparison between the graphite foam heat exchangers and the louvered fin heat exchanger, the inlet air speed is ranging from 5 m/s to 15 m/s, which is based on the velocity of vehicles (18 km/h to 54 km/h). In this case, the Reynolds number is ranging from 6400 to 19200. Thus turbulent flow prevails. However, it is still laminar flow inside the graphite foam. This is so, because it is difficult to generate turbulent eddies in the small open cells of the foam.

2.3 Computational domain

In order to get a uniform air velocity profile at the entrance, the computational domain is extended upstream 1.5 times the graphite foam length. On the other hand, to eliminate the outlet influence on the flow inside the graphite foam, the computational domain is also extended downstream 5 times the length of the graphite foam. Thus, the whole stream length of the computational domain is 7.5 times the actual graphite foam length.

3 MATHEMATICAL FORMULATION AND NUMERICAL METHOD

3.1 Governing equations

According to the presented assumptions, the governing equations for continuity, momentum and energy can be expressed as follows, see [13]:

Continuity equation

$$\frac{\partial u_i}{\partial x_i} = 0 \quad (i = 1, 2, 3) \tag{1}$$

Momentum equations

$$\rho_{eff} \frac{\partial}{\partial x_i}\left(u_i u_k\right) = \mu_{eff} \frac{\partial}{\partial x_i}\left(\frac{\partial u_k}{\partial x_i}\right) - \frac{\partial P}{\partial x_k} + S_i \quad (i = 1, 2, 3; k = 1, 2, 3) \tag{2}$$

Energy equation

$$\rho_{eff} c_{p.eff} \frac{\partial}{\partial x_i}\left(u_i T\right) = k_{eff} \frac{\partial}{\partial x_i}\left(\frac{\partial T}{\partial x_i}\right) \quad (i = 1, 2, 3) \tag{3}$$

There are some parameters which need to be specified. Based on the comparison between the momentum equations (Eq. 2) and the one in [14], it should be noted that:

(1) The effective density is: $\rho_{eff} = \dfrac{\rho_f}{\varepsilon}$;

(2) The effective viscosity is: $\mu_{eff} = \dfrac{\mu_f}{\varepsilon}$;

(3) The effective specific heat is: $c_{p.eff} = \varepsilon c_{p.f} + (1-\varepsilon) c_{p.s}$;

(4) The source term is: $S_i = -\left(\dfrac{\mu_f}{\alpha} u_i + \dfrac{\rho_f C_F}{\sqrt{\alpha}} |u| u_i \right)$, which is based on the Forchheimer extended Darcy's equation.

The effect of turbulence on the flow field is implemented by the "renormalization group" (RNG) k-ε turbulence model, which is more accurate by including the effect of swirl effect. On the other hand, due to the laminar flow inside the graphite foam, the RNG k-ε turbulence model might be useful to take into account low - Reynolds - number effects near the foam walls. The transport equations of the turbulence kinetic energy (k) and its dissipation rate (ε) can be found in [15].

3.2   Boundary conditions
The necessary boundary conditions for the three regions are as follows:
(1) At the upstream extended region (domain inlet)
- At the inlet: $u = const$, $T = const$, $v = w = 0$
- At the upper and lower boundaries: $\dfrac{\partial u}{\partial z} = \dfrac{\partial v}{\partial z} = 0$, $w = 0$, $\dfrac{\partial T}{\partial z} = 0$
- At the right and left sides: $\dfrac{\partial u}{\partial y} = \dfrac{\partial w}{\partial y} = 0$, $v = 0$, $\dfrac{\partial T}{\partial y} = 0$

(2) At the downstream extended region (domain outlet)
- At the upper and lower boundaries: $\dfrac{\partial u}{\partial z} = \dfrac{\partial v}{\partial z} = 0$, $w = 0$, $\dfrac{\partial T}{\partial z} = 0$
- At the right and left sides: $\dfrac{\partial u}{\partial y} = \dfrac{\partial w}{\partial y} = 0$, $v = 0$, $\dfrac{\partial T}{\partial y} = 0$
- At the outlet boundary: $\dfrac{\partial u}{\partial x} = \dfrac{\partial v}{\partial x} = \dfrac{\partial w}{\partial x} = \dfrac{\partial T}{\partial x} = 0$

(3) At the foam region
- At the upper and lower boundaries: $\dfrac{\partial u}{\partial z} = \dfrac{\partial v}{\partial z} = 0$, $w = 0$, $\dfrac{\partial T}{\partial z} = 0$
- At the right and left sides: $u = v = w = 0$, $T_w = const$

3.3   Numerical method
The commercial code ANSYS FLUENT 12.0 is used for the numerical solution. A control-volume-based technique is adopted to convert the governing equations to algebraic equations so that they can be solved numerically [16]. The SIMPLE algorithm is used to couple pressure and velocity. A second-order upwind scheme is used for the space discretization of the momentum and energy equations in the simulations. The residuals of the continuity, components of velocity are below 10^{-3}, while for energy it is below 10^{-6}.

The hexagon mesh is generated by using the blocking technique in ICEM. In order to check the grid independence, several sets of the mesh size have been adopted. For instance, three sets of the mesh size (63-79-12, 63-93-12, 63-93-20) were selected to check the grid independence of the corrugated foam. It is found that the variation of pressure drop is between 2-2.7 %, and the variation of Nusselt number is between 0.2-

0.3 %. Thus, the mesh size of 63-93-12 was adopted for the corrugated foam simulations. The same method is adopted to check the grid independence of the other foam configurations.

3.4 Calculation of performance parameters

For given conditions, the thermal performance of the graphite foam can be characterized by the Nusselt number (Nu).

$$\mathrm{N}u = \frac{h\,D}{k_f} = \frac{D}{k_f A}\frac{Q_{removed}}{\Delta T} = \frac{D_h}{k_f A_b}\frac{Q_{removed}}{\Delta T} \tag{4}$$

In Eq. (4), D is a characteristic length scale which is based on either the equivalent particle diameter of the foam or the hydraulic diameter of the channel. A is the area, which is the effective heat transfer surface or the heated base area of the foam. In order to simplify Eq. (4), D is defined as the hydraulic diameter of the channel D_h, A is the heated base area A_b, and $\triangle T$ is the mean temperature difference between the heated base and the fluid inlet temperature.

On the other hand, the definition of COP is how much heat can be removed by a certain input pump power; PD: how much heat can be removed by a certain mass of fins; and CF: how much heat can be removed in a certain volume. Thus, these parameters are defined as follows:

$$COP = \frac{Q_{removed}}{P_{pum}} = \frac{Q_{removed}}{u_{in}A_{in}\Delta P} \tag{5}$$

$$PD = \frac{Q_{removed}}{1000 \cdot m_{HEX}} \tag{6}$$

$$CF = \frac{Q_{removed}}{1000 \cdot V_{HEX}} \tag{7}$$

4 RESULTS AND DISCUSSION

4.1 Verification of the simulation model

Before presenting the results of the four configurations of the foam, it is necessary to test the simulation model of the graphite foam. Thus, a block graphite foam with size of 6 mm (width) x 50 mm (height) x 50 mm (length) was simulated. The pressure drop and Nu number were compared with the experimental results [9], as shown in Figs. 2 and 3.

The pressure drop values of the present simulation model are justified to be comparable to [9], as shown in Fig. 2. However, the Nusselt numbers (as shown in Fig. 3) of the present simulation model are slightly higher than the experimental results in [9]. It might be attributed to the effective specific heat ($c_{p.eff}$) of the graphite foam. There was no data about the effective specific heat ($c_{p.eff}$) of the graphite foam in [9]. However, according to [13], the effective specific heat of the graphite foam in the simulation is calculated as $c_{p.eff} = \varepsilon c_{p.f} + (1-\varepsilon)c_{p.s}$. Because of the effective specific heat of the

graphite foam, the difference in the Nusselt numbers between the present simulation and the experiment is somewhat high. However, when the fluid velocity is increased, the difference is reduced. Consequently, it is believed that the present simulation model is satisfactory to estimate the graphite foam pressure drop and the thermal performance.
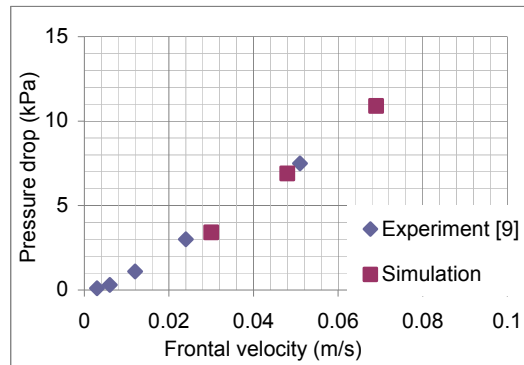

Fig. 2. Comparison of the pressure drop of the present simulation model with the experimental results in [9] (fluid is water).
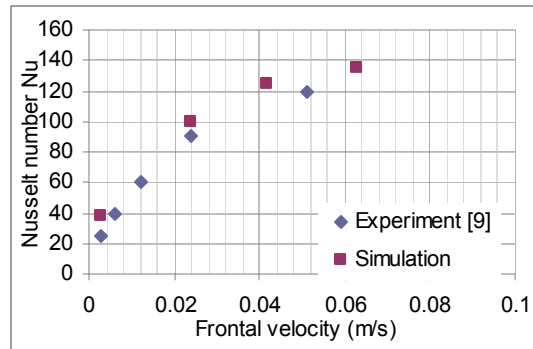

Fig. 3. Comparison of the Nusselt number of the present simulation model with the experimental results in [9].

4.2 Comparison between graphite foam and aluminum louver fin

Based on a lot of experimental research about the louver fin heat exchanger [17-18], the heat removed by the louver fin heat exchangers can be evaluated by the heat transfer correlation in [17], which was based on 91 samples of louver fin heat exchangers and the mean deviation was 7.55 %. The pressure drop can be evaluated by the friction correlation in [18], with a deviation of 9.21 % within the 91 samples. The results of COP, PD, and CF are shown in Figs. 4 to 6.

The louver fin heat exchanger has a larger COP value than the corrugated graphite foam heat exchangers, as shown in Fig. 4. With increasing air velocity, the COP of louver fin reduces much faster than that of the corrugated graphite foam. Thus, the louver fin has less superiority in COP compared to the corrugated graphite foam at high velocity. However, due to the high pressure drop through the corrugated graphite foam, large input pumping power is required. This causes the COP of the corrugated foam to be lower than that of the louver fin. If the corrugated foam can have the same COP as the louver fin, then the air velocity might be supersonic, based on Fig. 4. Thus, by increasing the air velocity to achieve the same COP as the louver fin, it is not feasible

for the corrugated foam.   Another possible method is to apply an appropriate configuration to the graphite foam, so that the flow length inside the graphite can be optimized. Due to the optimized flow length, the pressure loss can be reduced. In this case, the graphite foam heat exchanger might have similar COP as a convectional louver fin heat exchanger.

The PD value is higher for the corrugated graphite foam than for the aluminum louver fin. The PD values of these two heat exchangers are almost the same at low velocity (as shown in Fig. 5). With increasing velocity, the PD superiority of the corrugated graphite foam becomes more and more evident. This means that the corrugated graphite foam heat exchanger is much lighter than the louver fin heat exchanger, when the removed heat is the same. This is mainly attributed to the small density of the graphite foam.

Fig. 6 reveals that the CF value of the corrugated graphite foam is higher than that of the louver fin, especially at high velocity. It means that the graphite foam can dissipate more heat than the aluminum louver fin for the same volume. This is so, because there are many open cells in the graphite foam. Thus, the graphite foam can provide much larger heat transfer surface than the aluminum louver fin. In other words, the compactness of the corrugated foam is much higher than that of the aluminum louver fin. The heat exchanger with high compactness is very favorable in vehicle cooling systems, due to the space limitation in vehicles. Thus, the graphite foam has a high potential to reduce the size of the heat exchangers in vehicles.
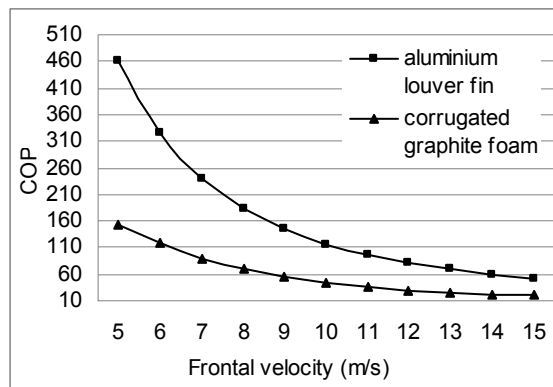

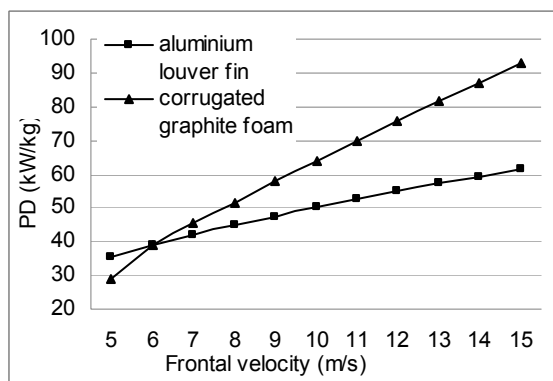Fig. 4. COP value of corrugated graphtie foam and louver fin.

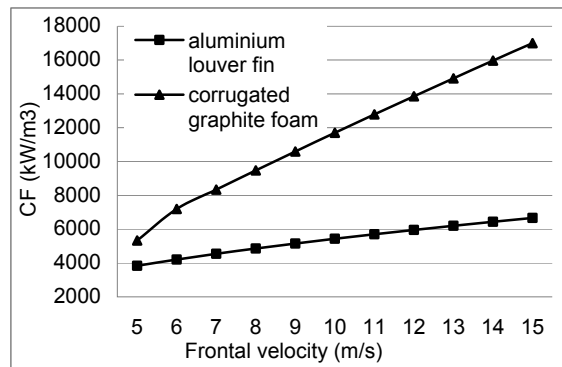Fig. 5. PD value of corrugated graphite foam and louver fin.

Fig. 6. CF value of corrugated graphite foam and louver fin.

5   CONCLUSION AND RECOMMENDATION

Due to the high thermal conductivity of graphite foam, the graphite foam is a potential candidate material for heat exchangers in vehicles. In order to evaluate the performance of graphite foam heat exchangers, a corrugated graphite foam is compared with a convectional aluminum louver fin. The major results are as follows:

1) The value of PD and CF are much higher in the corrugated graphite foam than in the aluminum louver fin. Thus, the graphite foam can reduce the weight and size of heat exchangers significantly, which would lead to a light or compact cooling system in vehicles.
2) The aluminum louver fin has a higher COP value than the corrugated graphite foams. By increasing the velocity, the difference in COP between the corrugated foam and aluminum louver fin heat exchangers becomes smaller.

Because the graphite foam is not a mature thermal material, there are still several problems (high pressure drop, low COP value, weak mechanical properties, and so on) blocking the development of graphite foam heat exchangers. Thus, much work has to be done before the graphite foam heat exchangers appear in vehicle cooling systems.

6   ACKNOWLEDGMENT

7   REFERENCES

1. Klett, J. W., "Process for Making Carbon Foam", US Patent 6033506, 2000.

2. Yu, Q., Thompson, B. E., and Straatman, A. G., "A Unit Cube-Based Model for Heat Transfer and Fluid Flow in Porous Carbon Foam", *Journal of Heat Transfer*, Vol. 128, pp: 352-360, 2006.

3. Straatman, A. G., Gallego, N. C., Thompson, B. E., and Hangan, H., "Thermal Characterization of Porous Carbon Foam - Convection in Parallel Flow", *International Journal of Heat and Mass Transfer*, Vol. 49, pp: 1991-1998, 2006.

4. Klett, J., Hardy, R., Romine, E., Walls, C., and Burchell, T., "High-thermal-conductivity, Mescophase-pitch-derived Carbon Foams: Effect of Precursor on Structure and Properties", *Carbon*, Vol. 38, pp: 953-973, 2000.

5. Paek, W. J., Kang, H. B., Kim, Y. S., and Hyum, M. J., "Effective Thermal Conductivity and Permeability of Aluminum Foam Materials", *International Journal of Thermophys*, Vol. 21 (2), pp: 453-464, 2000.

6. Klett, J., Ott, R., and McMillan, A., "Heat Exchangers for Heavy Vehicles Utilizing High Thermal Conductivity Graphite Foams", SAE Paper 2000-01-2207, 2000.

7. Yu, Q., Straatman, A. G., and Thompson, B. E., "Carbon-foam Finned Tubes in Air-water Heat Exchangers", *Applied Thermal Engineering*, Vol. 26, pp: 131-143, 2006.

8. Garrity, P. T., Klausner, J.F., and Mei, R., "Performance of Aluminum and Carbon Foams for Air Side Heat Transfer Augmentation", *Journal of Heat Transfer*, Vol. 132, 121901-(1-10), 2010.

9. Straatman, A. G., Gallego, N. C., Yu, Q., and Thompson, B. E., "Characterization of Porous Carbon Foam as a Material for Compact Recuperators", *Journal of Engineering for Gas Turbines and Power*, Vol. 129, pp: 326-330, 2007

10. Gallego, N. G., and Klett, J. W., "Carbon Foams for Thermal Management", *Carbon*, Vol. 41, pp: 1461-1466, 2003.

11. Leong, K. C., Jin, L. W., Li, H. Y., and Chai, J. C., "Forced Convection Air Cooling in Porous Graphite Foam for Thermal Management Applications", 11th Intersociety Conference on Thermal and Thermomechanical Phenomena in Electronic Systems, pp: 57-64, 2008.

12. Lin, Y. R., Du, J. H., Wu, W., Chow, L. C., and Notardonato, W., "Experimental Study on Heat Transfer and Pressure Drop of Recuperative Heat Exchangers Using Carbon Foam", *Journal of Heat Transfer*, Vol. 132, 091902-(1-10), 2010.

13. Yuan, J., Huang, Y., Sundén, B., and Wang, W., "Analysis of Parameter Effects on Chemical Reaction Coupled Transport Phenomena in SOFC Anodes", *Heat Mass Transfer*, Vol. 45, pp: 471-484, 2009.

14. Lu, W., Zhao, C. Y., and Tassou, S. A., "Thermal Analysis on Metal-foam Filled Heat Exchangers. Part I: Metal-foam Filled Pipes", *International Journal of Heat and Mass Transfer*, Vol. 49, pp: 2751-2761, 2006.

15. Pope, S. B., Turbulent Flows, Cambridge University, UK, 2000.

16. Versteeg, H. K., and Malalasekera, W., An Introduction to Computational Fluid Dynamics, second edition, Pearson Prentice Hall, UK, 2007.

17. Chang, Y., and Wang, C., "A Generalized Heat Transfer Correlation for Louver Fin Geometry", *International Journal of Heat and Mass Transfer*, Vol. 40, pp: 533-544, 1997.

18. Chang, Y., Hsu, K., Lin, Y., and Wang, C., "A Generalized Friction Correlation for Louver Fin Geometry", *International Journal of Heat and Mass Transfer*, Vol. 43, pp: 2237-2243, 2000.